



OPEN

## Nondestructive quantitative method for evaluation of magnesium hydroxide on surface of coated fabrics from Raman spectra

Jiří Militký<sup>1</sup>, Karel Kupka<sup>2</sup>, Dana Křemenáková<sup>1</sup>, Mohanapriya Venkataraman<sup>1</sup>✉, Juming Yao<sup>3</sup> & Guocheng Zhu<sup>3</sup>

Magnesium-based compounds, such as oxide ( $MgO$ ) and hydroxide ( $Mg(OH)_2$ ), are used in various applications ranging from medicine to electrotechnics. Especially, magnesium hydroxide coatings of textile structures are frequently used as part of flame retardant compositions, antibacterial agents, and surface absorption of far infrared radiation. Numerous analytical techniques exist for evaluating these compounds on material surfaces. The main aim of this article is to propose a novel methodology for the non-destructive quantitative evaluation of  $Mg(OH)_2$  coatings on the surfaces of typical synthetic fibers in low concentrations by analyzing Raman spectra. A regression approach was used to determine the concentration of  $Mg(OH)_2$  based on the assumption of Raman spectra additivity of  $Mg(OH)_2$  and the synthetic fiber. A simple modification of the sensor for analyzing Raman spectra was implemented, ensuring accurate positioning along all three axes. This methodology was applied to the analysis of polyester and polyamide textiles with  $Mg(OH)_2$  coatings.

**Keywords** Magnesium oxide, Magnesium hydroxide, Raman spectra, Textile coatings, Nondestructive technique

Magnesium oxide particles and nanoparticles are used in many application areas, such as agriculture (plant protection and growth support), biomedicine (bone regeneration), medicine (antimicrobial agents), electrotechnics (sensors, batteries), wastewater treatment (removal of toxic pollutants), and as flame retardants<sup>1</sup>. These particles possess a high melting point, low density, good mechanical properties, high thermal conductivity, self-cleaning activity (via photooxidation), high luminescence, and a high refractive index for photonic applications. They also exhibit low electrical conductivity, excellent optical transparency, and biocompatibility, among other beneficial properties<sup>2–5</sup>. Additionally, they are incorporated into compounds for so-called FIR (far infrared emitted) textiles, which can reuse infrared radiation emitted by humans for heating purposes<sup>6–9</sup>. The main application areas of  $MgO$  are illustrated in Fig. 1.

Magnesium oxide nanoparticles are sparingly soluble in water<sup>1</sup> and can easily be converted into magnesium hydroxide<sup>2</sup>. Magnesium hydroxide is also used as an antibacterial agent, flame retardant, and precursor for the production of magnesium oxide.  $Mg(OH)_2$  acts as a neutralizer for acidic wastewater and as a fertilizer<sup>2</sup>. Of particular interest are its various morphological forms, including needles, tubes, fibers, platelets, rods, and even “flower-like” shapes<sup>2</sup>.

Figure 1 shows the primary application areas of  $Mg(OH)_2$ . Numerous methods exist for synthesizing  $Mg(OH)_2$  and  $MgO$ , ranging from simple precipitation and calcination to chemical vapor deposition (see Fig. 2).

The use of coatings made from magnesium oxide and magnesium hydroxide and their possible combinations with ammonium polyphosphate in water dispersion for functional antibacterial finishing of textiles is described in the patent<sup>10</sup>. A simple method to fabricate multifunctional PET fabrics with excellent flame retardant and antibacterial properties based on functionalized  $Mg(OH)_2$  is described by Wang et al.<sup>11</sup>. They used nano- $Mg(OH)_2$  modified using titanate coupling agent and stearic acid to ensure better compatibility with PET fibers. Zhang et al. used  $Mg(OH)_2$  nanoparticles and polycarboxylic acid as cross-linkers for the surface coating of silk fabric to improve its flame retardancy and smoke suppression<sup>12</sup>.

<sup>1</sup>Department of Material Engineering, Faculty of Textile Engineering, Technical University Liberec, Liberec, Czech Republic. <sup>2</sup>TriloByte Statistical Software, Pardubice, Czech Republic. <sup>3</sup>Zhejiang-Czech Joint Laboratory of Advanced Fiber Materials, Zhejiang Sci-Tech University, Hangzhou 310018, China. ✉email: mohanapriya.venkataraman@tul.cz

MgO	Mg(OH) <sub>2</sub>
<ul style="list-style-type: none"> <li>•Antibacterial and anticorrosive agent</li> <li>•Fire-resistant and insulative material</li> <li>•Active absorbent of solid and gaseous impurities</li> <li>•Active catalyst support in organic reactions</li> <li>•Additive for the production of resistors and heating elements</li> <li>•Filler in paints, lacquers, and cement</li> <li>•Excipient ingredient in medicine</li> </ul>	<ul style="list-style-type: none"> <li>•Antibacterial agent</li> <li>•Neutralizer of water pollutants and liquid waste</li> <li>•Paper preservative</li> <li>•Component of membranes</li> <li>•Stabilizer for controlled release of biologically active proteins</li> <li>•Chemical sensor for ethanol</li> <li>•Additive for mechanical reinforcement of starch based bionanocomposite films</li> <li>•Flame retardant</li> </ul>

**Fig. 1.** Main applications areas of MgO and Mg(OH)<sub>2</sub> (adapted from<sup>2</sup>).

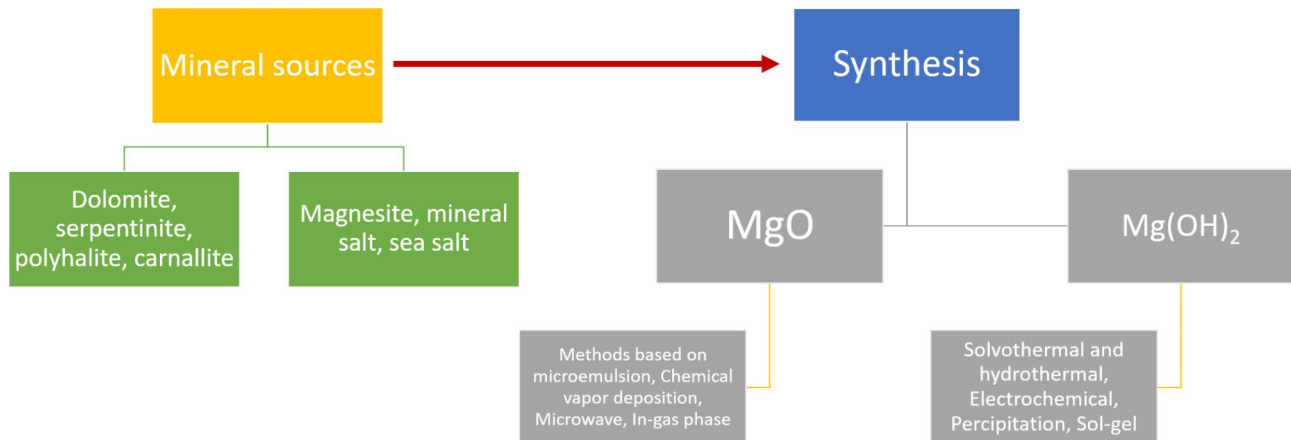


**Fig. 2.** Basic ways of Mg(OH)<sub>2</sub> and MgO preparation (adopted from<sup>2</sup> and<sup>13</sup>).

This report presents a methodology for the quantitative nondestructive evaluation of Raman spectra of typical synthetic fibers and Mg(OH)<sub>2</sub> coated on their surfaces in low concentrations. Regression analysis, based on the assumption of additivity of the spectra, was used to determine the concentration of this component. The developed methodology was applied to analyze polyester and polyamide textiles with Mg(OH)<sub>2</sub> surface deposits.

### Evaluation of Mg(OH)<sub>2</sub> content

For the qualitative indication of MgO and Mg(OH)<sub>2</sub>, spectroscopic techniques such as XRD, FTIR, and Raman spectroscopy are used<sup>14–16</sup>. The quantitative analysis of Mg(OH)<sub>2</sub> content is commonly based on titration.

Spectroscopic methods need to create calibration curves relating the intensity of the typical peak in spectra to known concentrations of  $\text{Mg}(\text{OH})_2$  powder often dissolved, e.g., in selected acids such as acetic acid. In the case of analysis of low concentrations of  $\text{Mg}(\text{OH})_2$  coated on the surface of fabrics, it is necessary first to extract this compound by using suitable chemicals as acids, which lead to the destruction of the coating. In these cases,  $\text{Mg}(\text{OH})_2$  particles frequently cover the fiber's surfaces only partially. To avoid the destruction of coating and laborious construction of calibration curves, it is possible to use a new simple method based on whole XRD, FTIR, or Raman spectra of the uncoated and  $\text{Mg}(\text{OH})_2$  coated fabric and spectra of pure  $\text{Mg}(\text{OH})_2$ . The amount of  $\text{Mg}(\text{OH})_2$  is calculated based on the assumption of spectra additivity. Raman spectroscopy, particularly micro-Raman spectroscopy, offers better spatial resolution, wider spectral coverage, narrower spectral bands, and lower water interference compared to XRD and FTIR spectroscopy<sup>17</sup>.

The Raman effect occurs when a sample is illuminated with monochromatic (laser) light, causing a small fraction of the scattered radiation to exhibit frequency shifts corresponding to the vibrational transitions of the material. Raman spectroscopy detects light scattered inelastically at frequencies different from the incident light, corresponding to molecular or lattice vibrations within the tested sample<sup>18,19</sup>. Raman scattering is the process of re-radiation of scattered light by dipoles induced in molecules by incident light, which is modulated by the vibrations of the molecules<sup>20</sup>. Therefore, the intensity of one peak in spectra is not sufficient for quantitative analysis of the sample because it corresponds to the presence of some groups only.

In normal Raman scattering, the dipoles are generated through the interaction between the electric field component (E) of the incident light and the molecules<sup>20</sup>. Raman scattering thus arises from the oscillatory polarization of the molecule as a function of its vibrations rather than from the molecule's permanent dipole. Molecules in the ground state produce bands shifted to lower energies than the incident light, while higher-frequency bands result from molecules in excited vibrational states. These bands originate from the material's inelastic scattering of light. Elastic collisions, on the other hand, result in Rayleigh scattering, which appears more intense than the unshifted component of the scattered light<sup>20</sup>.

## Materials and methods

### Fabrics

The knitted PAD 6,6 (hexamethylene adipate, fabric thickness 30 mm) and woven PET (polyethylene terephthalate, fabric thickness 32 mm) produced by Sintex Company Czechia and specified in Table 1 were used as starting material. Fiber surface roughness was evaluated by confocal laser microscope Olympus Lext 3000 (see Fig. 3). Illustrative images of both fabrics are in Fig. 3.

Before the actual coating, the surfaces of the PET fabric were activated using the following steps:

1. Hydrolytic cleaning in 5 wt%  $\text{H}_2\text{SO}_4$  for 30 min with stirring and then rinsing and drying at 140 °C for 2 min.
2. Washing in 1 wt% NaOH for 5 min and then rinsing.
3. Drying at 120 °C for 20 min.

Activation of PAD 6,6 textiles was carried out only by alkaline hydrolysis in 2% NaOH and 0.2% decyl glycoside solution at 50 °C for 30 min, followed by rinsing and centrifugation.

### Preparation of $\text{Mg}(\text{OH})_2$

A solution of 40 g of  $\text{MgSO}_4$  (P.A., Lach-Ner) was precipitated with an equivalent amount of NaOH. After vacuum filtration at 80 °C using a Büchner funnel, the precipitate was washed with distilled water and finally with isopropanol. It was then air-dried at 20 °C. The  $\text{Mg}(\text{OH})_2$  powder is shown in Fig. 4 (left).

### Preparation of $\text{MgO}$

The dried and homogenized  $\text{Mg}(\text{OH})_2$  was annealed at 900 °C for 5 min. The resulting  $\text{MgO}$  powder is shown in Fig. 4 (right).

### Coating

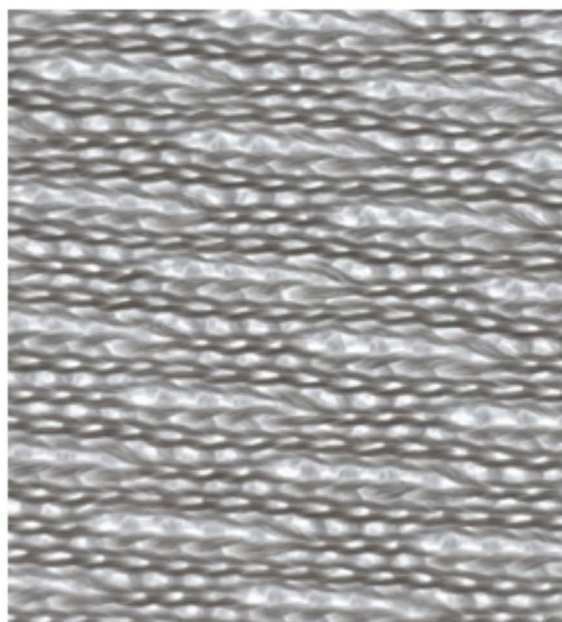
The methodology used for coating PET knitted fabric is described in the first column of Table 2. The methodology used for coating polyamide fabric is given in the second column of Table 2.

### Evaluation of Raman spectra

For the evaluation of Raman spectra, the Dual Lightnovo mini Raman spectrometer was used with excitation lasers of 785 nm and 660 nm, covering the spectral ranges of 2400–400  $\text{cm}^{-1}$  and 4000–2600  $\text{cm}^{-1}$ . Accompanying Miraspec communication software was used to acquire the spectra. To improve focus, a stand with micrometric XY shifts and coarse Z shift adjustment was constructed by the company Trilobyte (see Fig. 5).

Type	Material composition	Pattern	Areal density [ $\text{g m}^{-2}$ ]
PET	100% PES filament 82 dtex, knitted	Double face filet	143
PAD 6,6	100% PAD 6,6, filament 78 dtex, woven	Satin 5/1	105

**Table 1.** Material description.



**PET knitted**  
**(fiber mean surface roughness 0,22  $\mu$  m)**



**PAD 6,6 woven**  
**(fiber mean surface roughness 0,082  $\mu$  m)**

**Fig. 3.** Structure of starting fabrics.



**Fig. 4.** Powdered magnesium oxide (right) and hydroxide (left).

(PET)	(PAD 6,6)
1. Treatment of 20 × 20 cm samples in two liters of 0.02 M/l $Mg (NO_3)_2 \cdot 6H_2O$ solution for 30 min.	1. Treatment of 20 × 20 cm samples in two liters of 0.02 M/l $Mg (NO_3)_2 \cdot 6H_2O$ solution for 30 min.
2. Hydrolytic formation of $Mg (OH)_2$ by gradual addition of 0.04 M/l NaOH solution for 30 min.	2. Hydrolytic formation of $Mg (OH)_2$ by gradual addition of 0.04 M/l NaOH solution for 1 h.
3. Rinsing and centrifugation.	3. Rinsing and centrifugation.
4. Thermal stabilization in a thermopress at 150 °C for 30 min.	4. Thermal stabilization in a thermopress at 140 °C for 30 min.

**Table 2.** Textile coating procedure.

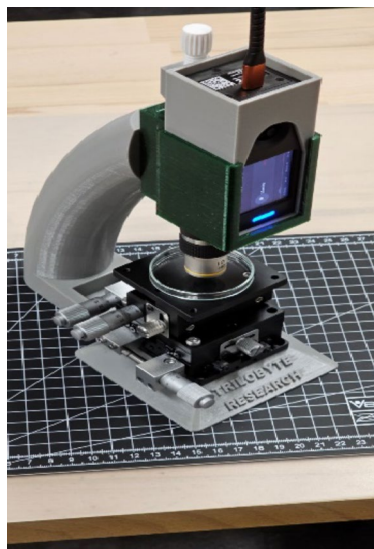


**Fig. 5.** Lightnovo mini Raman spectrometer is on stand with the XYZ shift.

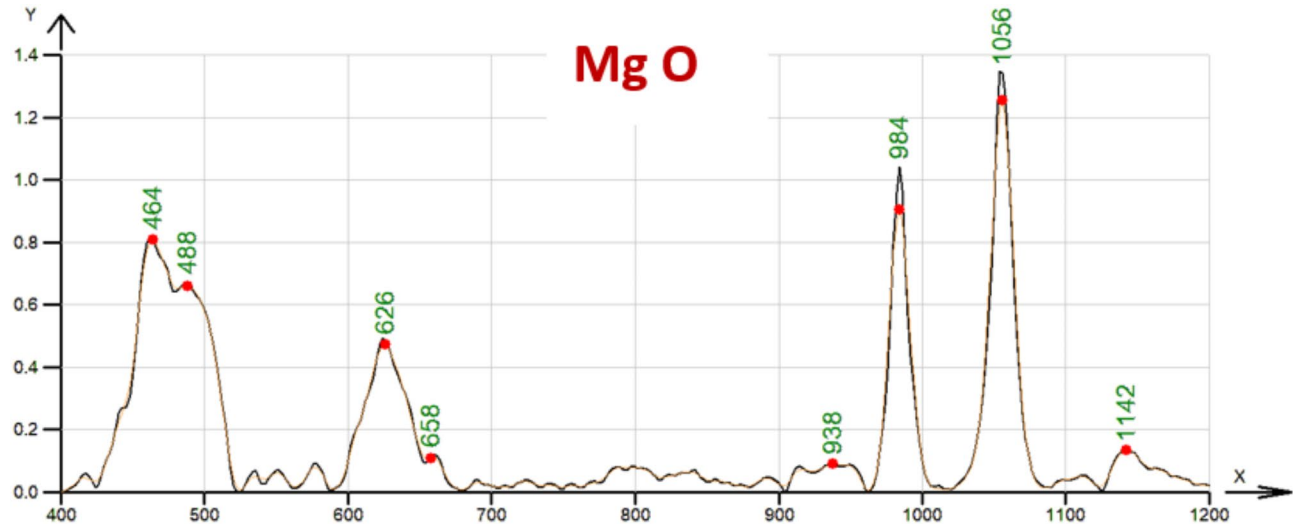


**Fig. 6.** Raman spectrum of MgO, excitation laser 785 nm.

## Results and discussion

All Raman spectra have a y-axis intensity [-] and x axis wavenumber [ $\text{cm}^{-1}$ ] as standard output from the spectrometer. Raman spectrum of MgO is shown in Fig. 6 and of  $\text{Mg}(\text{OH})_2$  in Fig. 7.

The Raman spectrum clearly distinguishes magnesium oxide from magnesium hydroxide by a very strong emission band at  $1056 \text{ cm}^{-1}$ , which is present in the oxide but absent in the hydroxide. The spectrum of  $\text{Mg}(\text{OH})_2$  has been utilized to detect the presence of hydroxide in coated textile fabrics.

Raman spectra in the Raman shift range of 400 to  $2400 \text{ cm}^{-1}$  for uncoated PAD 6,6 fabric are shown in Fig. 8, and for  $\text{Mg}(\text{OH})_2$  - coated PAD 6,6 fabric in Fig. 9.

Raman spectra in the Raman shift range of 400 to  $2400 \text{ cm}^{-1}$  of uncoated PET fabric are shown in Fig. 10, and for  $\text{Mg}(\text{OH})_2$  coated PET fabric is shown in Fig. 11.

The spectra of the uncoated and  $\text{Mg}(\text{OH})_2$  coated fabrics show no marked visible differences. Table 3 shows the strongest bands of the two fabrics (PAD 6,6 and PES).

Based on the availability or experimental spectra of uncoated fabric,  $\text{Mg}(\text{OH})_2$  coated fabric, and pure  $\text{Mg}(\text{OH})_2$ , it is possible to calculate the relative portion of uncoated fabric and magnesium hydroxide without the necessity to create calibration curves.

Assuming the additivity of Raman spectra, the spectrum of a mixture of two substances, in the absence of chemical interaction between them, can be expressed as a linear combination of the spectra of the individual substances. For the case where Raman spectra of coated fabric ( $R_C$ ), uncoated fabric ( $R_U$ ), and pure  $\text{Mg}(\text{OH})_2$  ( $R_M$ ) are at disposal (measured), the following relationship can be used:

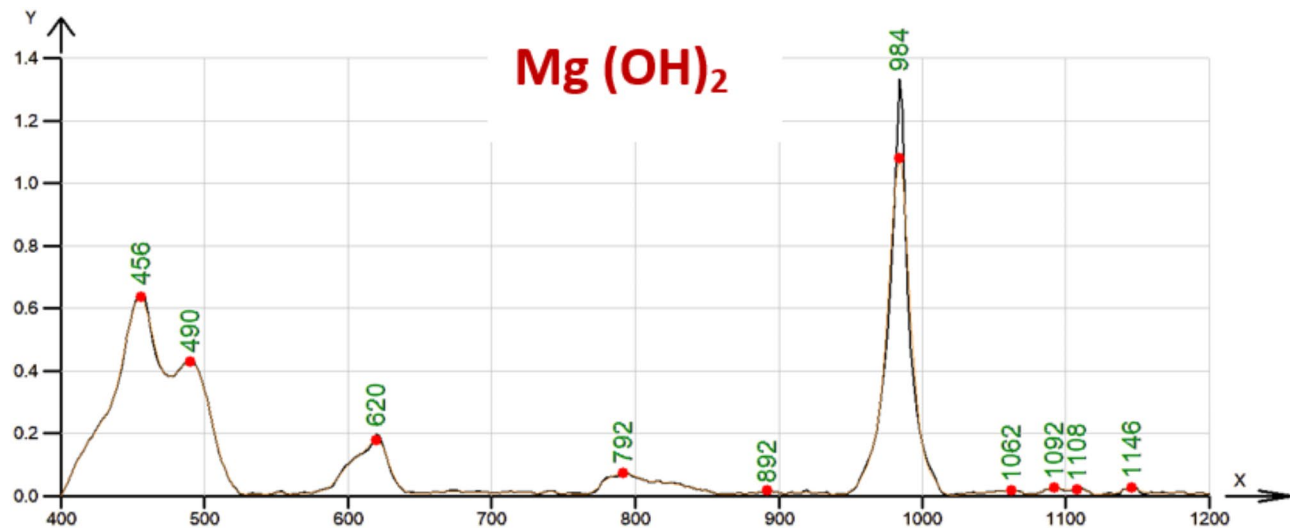


**Fig. 7.** Raman spectrum of Mg(OH)<sub>2</sub>, excitation laser 785 nm.

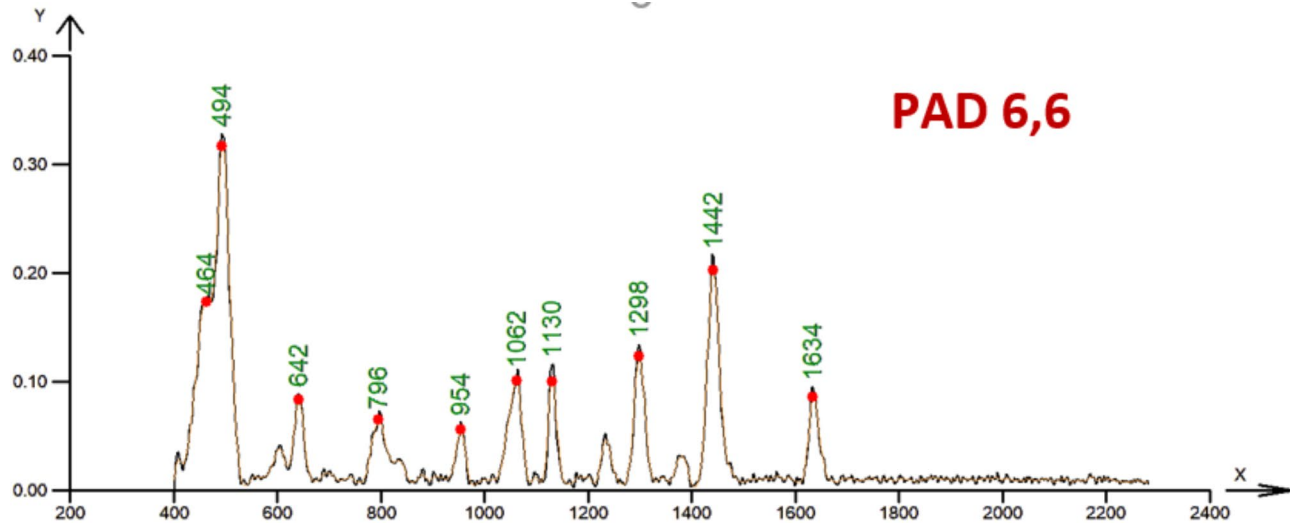


**Fig. 8.** Raman spectrum of uncoated PAD 6,6 fabric, excitation laser 785 nm.

$$R_C = a \cdot R_U + b \cdot R_M \quad (1)$$

Here,  $a$  represents the relative proportion of the uncoated fabric, and  $b$  represents the relative proportion of Mg(OH)<sub>2</sub> (proportional to the percentages of their relative concentration). These parameters can be calculated from the whole spectrum, i.e., at all measured wavenumbers (frequencies).

It is, therefore, possible to predict the Raman spectrum of coated fabric using a linear regression model, where  $a$  and  $b$  are the regression coefficients estimated using the ordinary least squares (OLS) method (see<sup>21</sup>).

Table 4 summarizes the results of the OLS analysis for PAD 6,6 coated with Mg(OH)<sub>2</sub>. For the characterization of the significance of parameters, the P values corresponding to each parameter estimate were calculated. This value P is the smallest significance level at which the null hypothesis  $H_0$  (estimated parameter is zero) is still rejected based on the given data. Denote that for confidence intervals, the significance level is equal to 0.05.

The results of OLS for PET coated by Mg(OH)<sub>2</sub> are summarized in Table 5.

A detailed description of the calculation and interpretation of these characteristics is provided in<sup>21</sup>.

The coefficient of determination  $R^2$  was selected as a characteristic of overall model quality<sup>21</sup>. It is well known that the predictive linear model (1) describes experimental data precisely (the sum of squared deviations between predicted values of Raman intensity and predicted values is approaching zero). In the case of coated PAD 6,6 fabric,  $R^2 = 0.92$  was calculated, and for coated PET fabric,  $R^2 = 0.94$  was calculated.

For the tested coated PAD 6,6 fabric, the concentration of Mg(OH)<sub>2</sub> was found to be 0.802%, while for the tested PET fabric, it was determined to be 4.715%. These values closely match the results obtained through titration of extracted Mg(OH)<sub>2</sub> using HCl (a destructive method) with NaOH and methyl orange as an indicator.

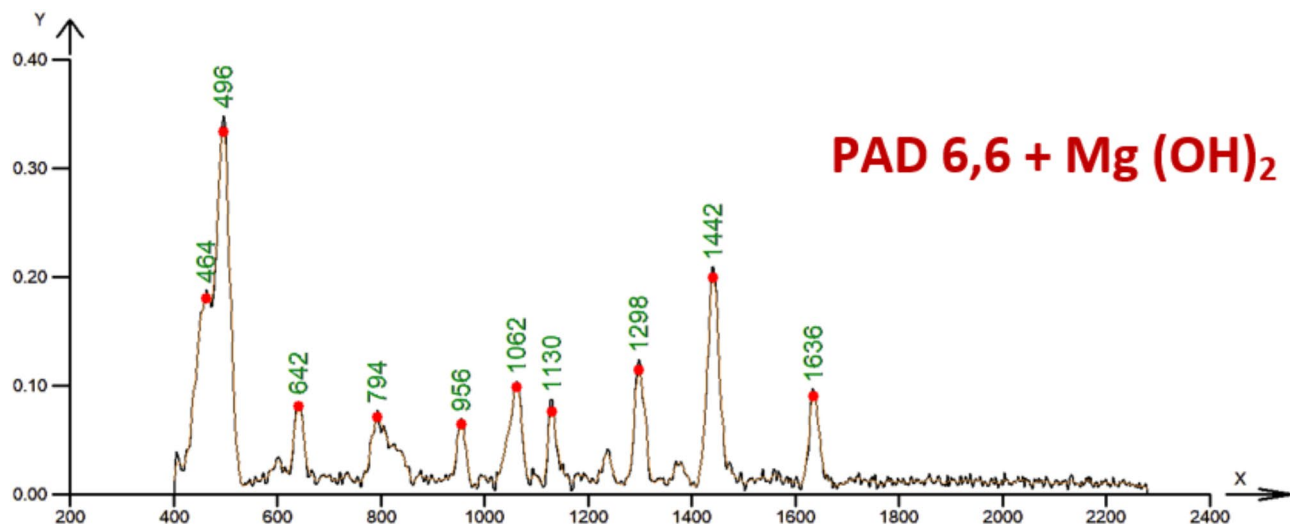


**Fig. 9.** Raman spectrum of PAD 6,6 fabric coated by  $\text{Mg}(\text{OH})_2$ , excitation laser 785 nm.

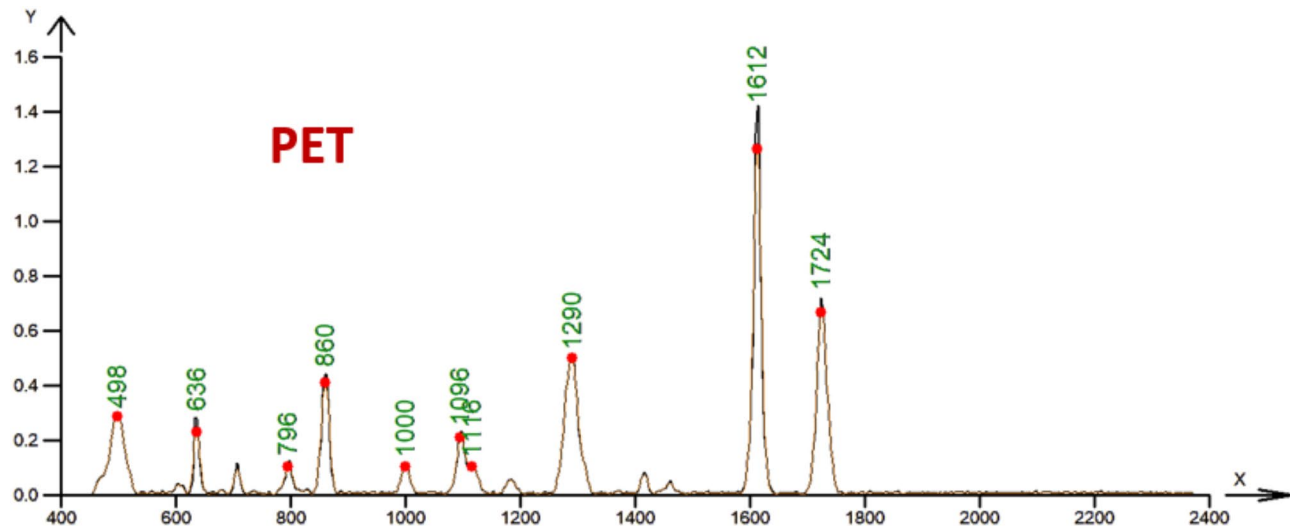


**Fig. 10.** Raman spectrum of uncoated PET fabric, excitation laser 785 nm.

The titration revealed an  $\text{Mg}(\text{OH})_2$  concentration of 0.44% for the coated PAD 6,6 fabric and 4.30% for the coated PET fabric.

If heteroskedasticity in the noise distribution is considered—since noise may have greater variance at higher signal intensities—it may be more appropriate to use the weighted least squares method with weights inversely proportional to the signal intensity. The set of tests for the characterization of peculiarities of experimental errors of measured spectra and corresponding changes of OLS criterion are described in the book<sup>21</sup>.

### Conclusions

Utilization of  $\text{Mg}(\text{OH})_2$  is very common in plenty of applications. It ranges from thermochemical energy storage<sup>22</sup> and shape-stabilized phase change materials<sup>23</sup> to  $\text{CO}_2$  adsorption at room temperature<sup>24</sup> and hydration of  $\text{Mg}(\text{OH})_2$  in reactive cement<sup>24–26</sup>. In the case of using coatings as a full surface layer or partial covering surface in the case of porous materials, it is necessary not only to identify the presence of  $\text{Mg}(\text{OH})_2$  but also concentration because it is directly related to changes of some properties. This task is not easy and obviously needs the construction of a calibration curve for the prediction of concentration from the measured signals. For high concentrations of  $\text{Mg}(\text{OH})_2$  powder, it is often sufficient to use image analysis of SEM images. A very low (few percent) content of  $\text{Mg}(\text{OH})_2$  in surface coatings cannot be easily identified visually by using SEM images. More sensitivity for the presence of  $\text{Mg}(\text{OH})_2$  in the coating is used in spectral methods such as Fourier transform infrared analysis (FTIR) or Raman spectroscopy, which is less sensitive to water content and the presence of colored substances. The linear regression-based method outlined herein is direct, uncomplicated, and requires no calibrations.

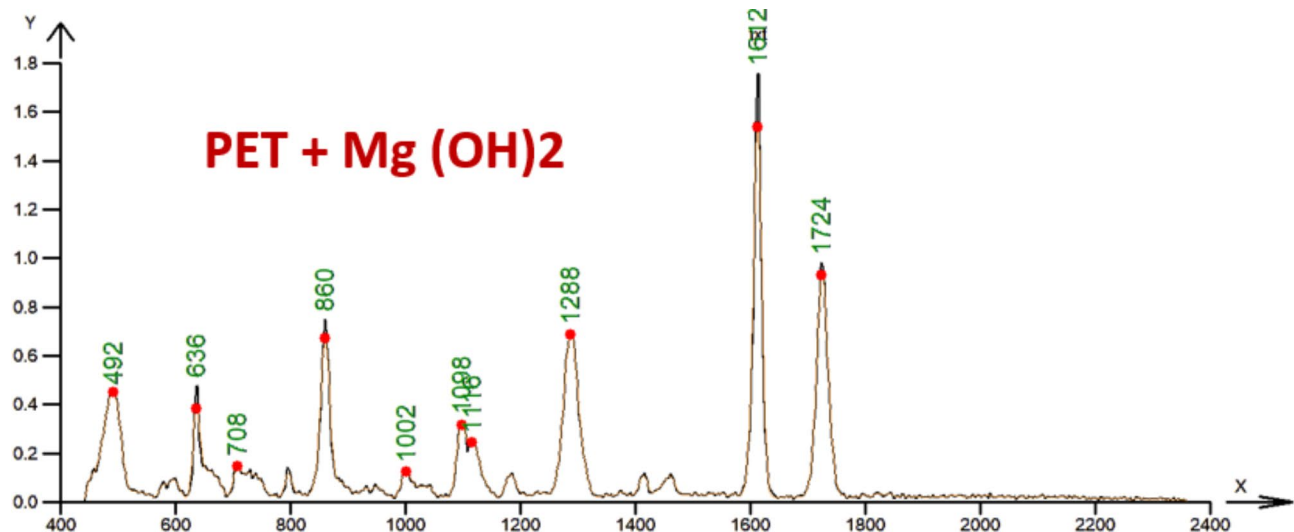


**Fig. 11.** Raman spectrum of PET fabric coated by  $\text{Mg}(\text{OH})_2$ , excitation laser 785 nm.

Type	The most significant Raman bands ( $\text{cm}^{-1}$ )
PAD 6,6	494, 1442, 464, 1298, 1062, 1130, 1634, 642, 796, 954
PET	1612, 1724, 1290, 860, 498, 636, 1096, 796, 1116, 1000

**Table 3.** The most significant Raman bands for PAD 6,6 and PES) fabrics.

Parameter	Estimator	Standard deviation	P value	Conclusion	Confidence interval
Intercept	0.00214	0.00025	0	Significant	(0.00165, 0.00264)
a	0.99146	0.00502	0	Significant	(0.98161, 1.00131)
b	0.00802	0.00199	0.00006	Significant	(0.00412, 0.01193)

**Table 4.** Parameter estimates for PAD 6,6 coated by  $\text{Mg}(\text{OH})_2$ .

Parameter	Estimator	Standard deviation	P value	Conclusion	Confidence interval
Intercept	0.02986	0.00144	0	Significant	(0.02704, 0.03268)
a	1.29929	0.00909	0	Significant	(1.28146, 1.31712)
b	0.04715	0.01093	0.0002	Significant	(0.02569, 0.0686)

**Table 5.** Parameter estimates for PET coated by  $\text{Mg}(\text{OH})_2$ .

A verified methodology for the nondestructive evaluation of coated  $\text{Mg}(\text{OH})_2$  on different fibrous materials, based on Raman spectra and standard regression analysis, is novel, straightforward, and can replace more complex other analytical techniques. A simple modification of the Lightnovo mini Raman spectrometer into a specialized Raman microscope can serve as a cost-effective alternative to expensive Raman spectrophotometers. This method can be forecasted to support the use of  $\text{Mg}(\text{OH})_2$  in many applications and will serve as a tool for the optimization of its concentration.

## Data availability

All data generated or analyzed during this study are included in this published article.

Received: 5 March 2025; Accepted: 4 April 2025

Published online: 12 April 2025

## References

1. Fernandes, M. et al. Applications of magnesium oxide ( $\text{MgO}$ ) nanoparticles in various domains. *Adv. Mater. Lett.* **11**, 1–10 (2020).

2. Pilarska, A. A. et al. Recent development in the synthesis, modification and application of Mg (OH)<sub>2</sub> and MgO: A review. *Powder Technol.* **319**, 373–407 (2017).
3. Muhaymin, A. et al. Green synthesis of magnesium oxide nanoparticles using hyphaene Thebaica extract and their photocatalytic activities. *Sci. Rep.* **14**, 20135. <https://doi.org/10.1038/s41598-024-71149-0> (2024).
4. Tellez, P. & Waldron, J. R. Reflectance of magnesium oxide. *J. Opt. Soc. Am.* **45**, 19–22 (1955).
5. Abinaya, S. et al. Green synthesis of magnesium oxide nanoparticles and its applications: A review. *Sustain. Chem. Pharm.* **19**, 100368 (2021).
6. Hardy, J. & DuBois, D. (ed F, E.) Regulation the heat loss the from the human body. *Physiol. Proc. N S* **23** 624–631 (1937).
7. Hardy, J. D. The radiation of heat from the human body IV. *J. Clin. Invest.* **13**, 817–831 (1934).
8. Hardy, J. D. The radiation of heat from the human body V. *J. Clin. Invest.* **14**, 1–9 (1934).
9. Miličký, J. et al. A review of textiles reflecting FIR produced by the human body. *AUTEX Res. J.* **22**, 264–271 (2022).
10. Abuelhaiga, M. et al. Use of aqueous dispersions of magnesium compounds for functional finishing of textiles, world patent WO 2021/199049 A1, (2021).
11. Wang, Y. et al. Preparation of Nano-Mg (OH)<sub>2</sub> and its flame retardant and antibacterial modification on polyethylene terephthalate fabrics. *Polymers* **15**, 7. <https://doi.org/10.3390/polym15010007> (2023).
12. Zhang, C. et al. Preparation of nano-Mg (OH)<sub>2</sub> for surface coating of silk fabric with improved flame retardancy and smoke suppression. *Colloids Surf. A* **625**, 126868 (2021).
13. Verma, R. et al. Morphology, mechanism and optical properties of nanometer-sized MgO synthesized via facile wet chemical method. *Mater. Chem. Phys.* **148**, 1064–1070 (2014).
14. Ebinaga, T. et al. Influence of MgO powder addition on formation of MgO from Mg (OH)<sub>2</sub> by thermal decomposition. *Trans. Mater. Res. Soc. Jpn.* **35**, 373–376 (2010).
15. Kondo, A. et al. Investigation on the mechanisms of Mg (OH)<sub>2</sub> dehydration and MgO hydration by near-infrared spectroscopy. *J. Phys. Chem. C* **125**, 10937–10947 (2021).
16. Maltseva, A. et al. Effect of pH on Mg (OH)<sub>2</sub> film evolution on corroding Mg by in situ kinetic Raman mapping (KRM). *Corros. Sci.* **153**, 272–282 (2019).
17. Ren, L. et al. Identification of microplastics using a convolutional neural network based on micro-Raman spectroscopy. *Talanta* **260**, 124611 (2023).
18. Rebollar, E. et al. Physicochemical modifications accompanying UV laser induced surface structures on Poly (ethylene terephthalate) and their effect on adhesion of mesenchymal cells. *Phys. Chem. Chem. Phys.* **16**, 17551–17559 (2014).
19. Yoshikawa, M. *Advanced Optical Spectroscopy Techniques for Semiconductors* (Springer Nature, 2023).
20. Koenig, J. L. *Infrared and Raman Spectroscopy of Polymers* (RAPRA, 2001).
21. Meloun, M. & Miličký, J. Statistical data analysis. (Woodhead, 2011).
22. Miller, N. et al. The effect of the salt precursor on the particle morphology and thermal properties of magnesium hydroxide for thermochemical energy storage. *J. Energy Storage* **44**, 103335 (2021).
23. Zahir, H. et al. Shape-stabilized phase change materials for solar energy storage: MgO and Mg (OH)<sub>2</sub> mixed with polyethylene glycol. *Nanomaterials* **9**, 1773 (2019).
24. Senevirathna, H. L. et al. Counter-Intuitive Magneto-Water-Wetting effect to CO<sub>2</sub> adsorption at room temperature using MgO/Mg (OH)<sub>2</sub> nanocomposites. *Materials* **15**, 983 (2022).
25. Leblanc, L. L. *Filled Polymers: Science Industrial Applications* (CRC, 2010).
26. Gardeh, M. G. et al. Exploring mechanisms of hydration and carbonation of MgO and Mg (OH)<sub>2</sub> in reactive magnesium oxide-based cements. *J. Phys. Chem. C* **126**, 6196–6206 (2022).

## Acknowledgements

This work was supported by the project 'Advanced Structures for Thermal Insulation in Extreme Conditions' (reg. no. 21-32510 M) granted by the Czech Science Foundation (GACR).

## Author contributions

Conceptualization, Jiří Miličký and Mohanapriya Venkataraman; Data curation, Karel Kupka; Formal analysis, Mohanapriya Venkataraman; Funding acquisition, Jiří Miličký; Investigation, Karel Kupka, Dana Křemenáková and Guocheng Zhu; Methodology, Karel Kupka and Dana Křemenáková; Project administration, Jiří Miličký; Resources, Dana Křemenáková, Mohanapriya Venkataraman, Juming Yao and Guocheng Zhu; Software, Karel Kupka; Supervision, Jiří Miličký; Validation, Dana Křemenáková and Juming Yao; Visualization, Dana Křemenáková, Mohanapriya Venkataraman, Juming Yao and Guocheng Zhu; Writing – original draft, Jiří Miličký and Karel Kupka; Writing – review & editing, Mohanapriya Venkataraman.

## Funding

This work is funded by the Department of Material Engineering, Faculty of Textile Engineering, Technical University of Liberec, Czech Republic.

## Declarations

### Competing interests

The authors declare no competing interests.

### Additional information

Correspondence and requests for materials should be addressed to M.V.

Reprints and permissions information is available at [www.nature.com/reprints](http://www.nature.com/reprints).

**Publisher's note** Springer Nature remains neutral with regard to jurisdictional claims in published maps and institutional affiliations.

**Open Access** This article is licensed under a Creative Commons Attribution-NonCommercial-NoDerivatives 4.0 International License, which permits any non-commercial use, sharing, distribution and reproduction in any medium or format, as long as you give appropriate credit to the original author(s) and the source, provide a link to the Creative Commons licence, and indicate if you modified the licensed material. You do not have permission under this licence to share adapted material derived from this article or parts of it. The images or other third party material in this article are included in the article's Creative Commons licence, unless indicated otherwise in a credit line to the material. If material is not included in the article's Creative Commons licence and your intended use is not permitted by statutory regulation or exceeds the permitted use, you will need to obtain permission directly from the copyright holder. To view a copy of this licence, visit <http://creativecommons.org/licenses/by-nc-nd/4.0/>.

© The Author(s) 2025